

# Active sound transmission control of a double-panel module using decoupled analog feedback control: Experimental results

Jason D. Sagers

*Applied Research Laboratories, The University of Texas at Austin, Austin, Texas 78758*

Timothy W. Leishman

*Department of Physics and Astronomy, Brigham Young University, Provo, Utah 84602*

Jonathan D. Blotter

*Department of Mechanical Engineering, Brigham Young University, Provo, Utah 84602*

(Received 14 May 2010; accepted 21 August 2010)

Low-frequency sound transmission through passive lightweight partitions often renders them ineffective as means of sound isolation. As a result, researchers have investigated actively controlled lightweight partitions in an effort to remedy this problem. One promising approach involves active segmented partitions (ASPs), in which partitions are segmented into several distinctly controlled modules. This paper provides an experimental analysis of a double-panel ASP module wherein the source- and transmitting-side panels are independently controlled by an analog feedback controller. Experimental results, including plant frequency response functions, acoustic coupling strengths, frequency response functions, and transmission losses (TLs) of single- and double-panel modules, are presented and compared to numerical predictions. Over the bandwidth of 20 Hz to 1 kHz, the average measured TL for an actively controlled single-panel module was 29 dB, compared to 14 dB for the passive case. The average measured TL over the same bandwidth for the actively controlled double-panel module was 57 dB, compared to 31 dB for the passive case.

© 2010 Acoustical Society of America. [DOI: 10.1121/1.3488674]

PACS number(s): 43.40.Vn, 43.50.Ki, 43.55.Rg [BSC]

Pages: 2807–2816

## I. INTRODUCTION

Passive single- and double-panel partitions have long been used to reduce sound transmission into noise-sensitive environments. Although both types of partitions can provide reasonable sound isolation at high frequencies, their performance at low frequencies is severely degraded due to resonance effects.<sup>1,2</sup> A common passive method to reduce sound transmission is to add mass to the partition. In many applications, when weight is not an issue, this approach is fine. However, in many other applications, such as in aircraft cabins, rocket payload fairings, high-rise building walls, and large roofs and ceilings, this solution is not viable because of significant weight penalties. Active control has been proposed as a means of improving the low-frequency sound isolation of single- and double-panel partitions without adding much additional mass. Two of the active control approaches presented in the literature include active structural acoustic control (ASAC) and active segmented partitions (ASPs).

The term active structural acoustic control, or ASAC, was coined to describe a range of active control strategies wherein control forces are applied directly to a continuous panel in order to reduce radiated acoustic pressure.<sup>3</sup> The methods have been explored thoroughly.<sup>4–14</sup> In general, the receiving-side attenuations produced by single-panel ASAC methods have been modest (on the order of 5–10 dB). Performance comparisons of ASAC implementations have been difficult because the reported sound isolation measurement

techniques have been inconsistent. The major drawbacks to the ASAC approach include (1) large numbers of fully-coupled actuator/sensor pairs, (2) a frequent need for microphones in the receiving space, and (3) the spatial control spillover that inevitably results when controlling continuous panels. In short, the complexities of ASAC for large-scale implementations have been daunting.

An ASP provides an alternative to ASAC.<sup>15,16</sup> In this case, a single- or double-panel partition is subdivided into an array of discretely controlled modules that are mechanically and/or acoustically segmented from one another. When properly implemented, mechanical segmentation largely eliminates the spatial control spillover that occurs when trying to control a continuous panel. In the case of double-panel partitions, the interior space between the panels may also be acoustically segmented with an interstitial structure. The segmentation simplifies the control problem because individual module dimensions become small compared to the structural and acoustic wavelengths. It also reduces acoustic cross-talk between modules within the partition.

Leishman and Tichy produced theoretical and numerical models for two single-panel and two double-panel ASP modules.<sup>17</sup> The control objective for each was to minimize the surface velocity of the transmitting panel. Their most effective configuration was a double-panel arrangement in which a composite source-side panel was used to acoustically actuate the cavity (reducing the total volume velocity into the cavity) and thus control the transmitting panel. The

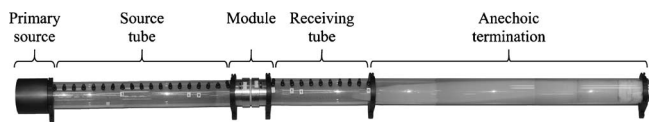


FIG. 1. Photograph of the TL measurement system.

normal-incidence TL of this type of module was measured in plane-wave tubes for both an individual module and a  $2 \times 2$  array of modules.<sup>18,19</sup> Using a digital feed-forward active noise control scheme, TL results near 80 dB were achieved over a band of 40 Hz to 1.0 kHz for the individual module and TL results near 55 dB were achieved over a band of 40 Hz to 300 Hz for the array of four modules. Both values were near the maximum measurable for the respective TL measurement systems.

Two drawbacks were identified with the aforementioned double-panel ASP module. First, the module used a feed-forward active controller. The time-advanced reference signal needed for feed-forward control is not available in many applications. In addition, the feed-forward controller was only capable of effectively attenuating tonal disturbances. For those applications in which an advanced reference signal is available and only tonal disturbances exist, the system would work well. However, since these conditions are not present in many sound isolation applications, an alternate approach is needed. Second, the method of volume velocity reduction in the system produced a unidirectional module: attenuation of sound was only possible in one direction. Many applications require bidirectional TL capabilities, wherein the module is capable of attenuating sound in both directions.

This paper presents experimental findings for a new double-panel ASP module, wherein the source- and receiving-side panels are directly sensed and actuated through a feedback controller.<sup>20,21</sup> The control scheme eliminates the need for time-advanced reference signals while minimizing the surface velocities of both panels (instead of just the transmitting panel), thus allowing bidirectional performance. The purpose of the paper is to present the experimental module configuration, the measurement system setup, and to report the experimental results for the new module. It is also to validate the numerical modeling results presented previously,<sup>20,21</sup> including frequency response functions (FRFs) for each plant, the acoustic coupling FRF between the panels, the TL in both passive and active states, and the bidirectional capabilities of the module.

## II. EXPERIMENTAL METHODS

### A. Measurement system

The plane-wave tube system shown in Fig. 1 was used to measure the normal-incidence TL of the new ASP module. The source and receiving tubes were both acrylic tubes with 10 cm inside diameters and airtight microphone ports located every 5 cm along their lengths. The primary excitation source was located at one end of the source tube and a 1.5 m anechoic termination was located at the far end of the receiving tube. The source consisted of a 10 cm full-range moving-coil driver with a sealed rear enclosure. The anechoic termi-

nation consisted of a tapered wedge cut from a solid cylinder of open-cell foam rubber and situated inside another section of 10 cm diameter acrylic tube. An air gap behind the wedge was filled with loose fiberglass insulation and the tube was capped with a thick steel plate. The module under test was mounted and sealed between the source and receiving tubes.

Because structural or acoustical flanking paths in the measurement apparatus might significantly affect the TL measurements, especially for modules with high TL, special steps were taken to reduce the strengths of those paths. The source tube was placed on a different table than the receiving tube to reduce structural flanking. The source tube was supported on a vibration isolation table which was also mounted on an isolated concrete slab. A resilient airtight connection was also used to join the two halves of the double-panel module so vibrational energy could not easily transmit directly through the module shell into the receiving tube.

The two-microphone transfer-function technique developed by Chung and Blaser<sup>22,23</sup> was used to measure the TL through the module. This provided a way to decompose the sound field in the source tube so that only the pressure incident upon the module was used in the TL calculations. The downstream field was also decomposed to reduce errors associated with any non-anechoic performance of the termination. Two microphone pairs were actually used on either side of the module: a pair with a larger spacing and a pair with smaller spacing. Each spacing determined the usable measurement bandwidth within desired error constraints.<sup>24</sup> A large spacing of 40 cm was used for one microphone pair with a corresponding usable bandwidth of 40 Hz to 345 Hz. A small spacing of 5 cm was used for the other microphone pair, with a corresponding usable bandwidth of 345 Hz to 2.7 kHz. The measurements associated with the two bandwidths were spliced together at 345 Hz to provide a composite measurement from 40 Hz to 2.7 kHz.

All microphones were placed at least 1.5 duct diameters away from the source or module to reduce the effects of evanescent cross modes in the respective acoustic near fields. The cutoff frequency for the first cross mode of the 10 cm diameter tube was approximately 2 kHz. Only plane waves propagated in the tube below this frequency, provided that the frequency content of the primary excitation source remained below 2 kHz. The excitation signal was white noise band-limited between 1 Hz and 2.0 kHz. Some cross modes would inevitably be excited during the measurements, but the amplitude of those modes would sufficiently evanesce as the waves reached the microphone locations.

Each microphone was calibrated to an absolute reference value (114 dB at 1 kHz), then a switching calibration routine was used to establish a frequency-dependent relative calibration between each microphone pair, in both magnitude and phase. Post-processing with the relative calibration removed the frequency-dependent characteristics of the microphones, preamplifiers, and the front-end of the data acquisition system for the two-microphone transfer-function technique.

The performance of the measurement system was substantiated in two ways. First, the frequency-dependent absorption coefficient of the anechoic termination was expected to approach a value of 1.0 above the anechoic cutoff fre-

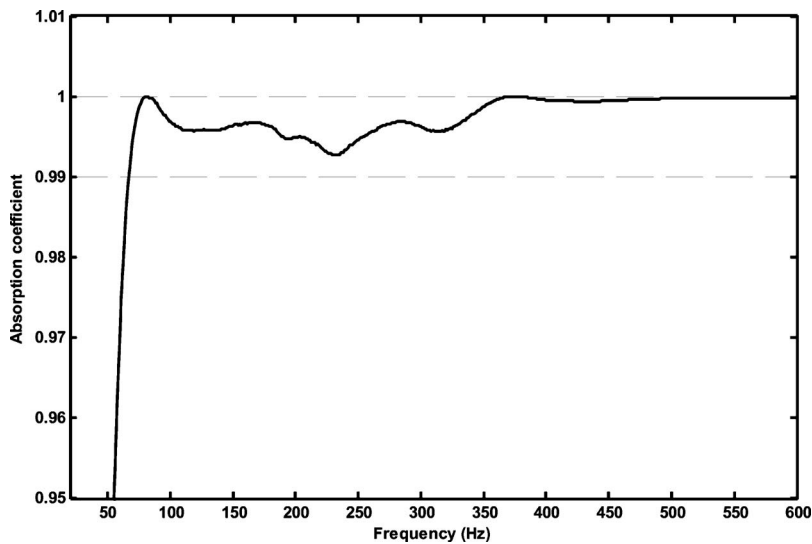


FIG. 2. Measured absorption coefficient for the 1.5 m anechoic termination. The dashed line at 0.99 represents the anechoic cutoff limit for the termination.

quency (the frequency above which the absorption coefficient consistently exceeds 0.99). The measured coefficient is shown in Fig. 2. The plot is zoomed into low frequencies and high absorption coefficient values to identify the cutoff frequency of approximately 67 Hz. However, the termination also provided an absorption coefficient exceeding 0.70 to 40 Hz or lower.

The second substantiation involved the TL measurement of another benchmark case without a completed module in place. The apparatus was arranged as if a typical TL measurement were to be conducted, but the actuators (loudspeakers) were removed from the module before the measurement. The TL through a section of air with the same length as the module should be nearly zero. The measured TL of this configuration is shown in Fig. 3, which shows that the measurement error introduced by the apparatus will be very small over the usable measurement bandwidth. The average error between 67 Hz and 1.8 kHz is 0.42 dB. It should be noted that slightly larger errors may be introduced below the 67 Hz anechoic termination cutoff frequency and at frequencies approaching the 2 kHz cutoff frequency of the first tube cross mode.

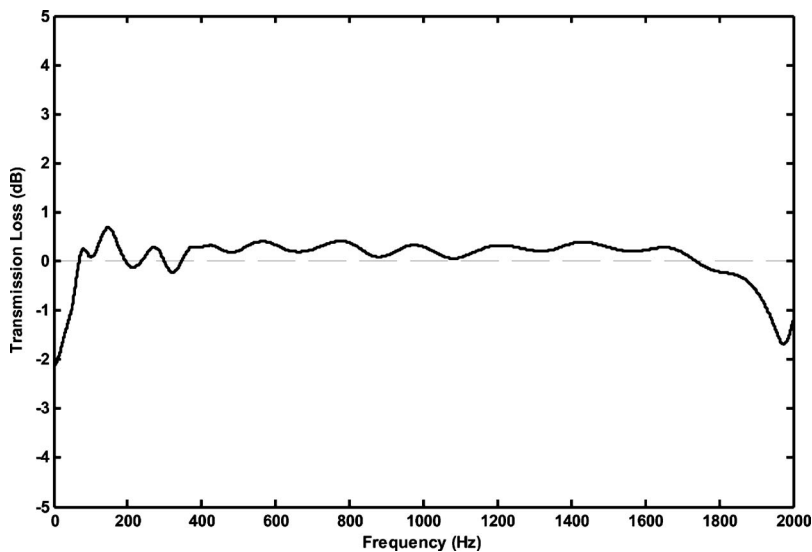


FIG. 3. TL of the measurement system without a module in place.

Both of the aforementioned tests provide some validation that the measurement apparatus was qualified to make accurate TL measurements between 67 Hz and 1.8 kHz. The experimental results immediately outside of these ranges could still be useful, but may have slightly larger levels of experimental error.

## B. Transducers

Several transducers were used with the experimental modules. The loudspeakers were 10 cm diameter HiVi M4N full-range drivers. The surface areas that comprised the cones and surrounds of the drivers made up the partition panels. The magnet and voice-coil assemblies provided the actuation of the panels. The measured Thiele-Small parameters and the extracted enhanced parameters<sup>20,21</sup> for this driver are shown in Table I.

Cutaway depictions of the experimental modules are shown in Fig. 4. A 0.7 g PCB 352B10 accelerometer was mounted to the center of each cone to sense its normal acceleration. Electrical connections to the loudspeaker terminals were made via airtight banana jacks. For the double-

TABLE I. Thiele-Small and enhanced parameters for the HiVi M4N loudspeaker.

Thiele-Small parameters		
Parameter	Value	Units
$BL$	3.54	Tm
$C_{MS}$	700	$\mu\text{m}/\text{N}$
$f_s$	83.1	Hz
$L_E$	0.23	mH
$M_{MD}$	5.43	g
$R_E$	6.48	$\Omega$
$R_g$	0.10	$\Omega$
$R_{MS}$	0.49	kg/s
$S_D$	54.1	$\text{cm}^2$
Enhanced parameters		
$BL$	3.54	Tm
$L_E$	0.23	mH
$R_E$	6.48	$\Omega$
$R_g$	0.10	$\Omega$
$S_1$	30.0	$\text{cm}^2$
$S_2$	3.00	$\text{cm}^2$
$M_{M1}$	7.21	g
$M_{M2}$	0.15	g
$C_{M1}$	2300	$\mu\text{m}/\text{N}$
$C_{M2}$	448	$\mu\text{m}/\text{N}$
$C_{M12}$	272	$\mu\text{m}/\text{N}$
$R_{M1}$	0.57	kg/s
$R_{M2}$	0.30	kg/s
$R_{M12}$	0.30	kg/s

panel module, the basket of each loudspeaker was oriented toward the interior of the cavity. A piece of fiberglass insulation (not shown) was inserted into the cavity to help damp the cavity resonances and provide greater passive TL at higher frequencies.

The microphones used in the measurement system were Larson Davis 377A02 precision microphones with Larson Davis PRM426 preamplifiers. The microphones were positioned along the length of the tube in the airtight microphone ports spaced at 5 cm intervals. All unused ports were sealed with plugs. A photograph of the receiving-side tube is shown in Fig. 5.



FIG. 5. Photograph of the receiving-side tube of the measurement system without a module attached. The microphone ports are spaced 5 cm apart and the tip of the anechoic wedge is visible near the end of the tube.

### C. Feedback controllers

Two identical Fleischer-Tow analog feedback controllers<sup>25</sup> were used in this research. The biquad circuit is a second-order filter whose response can be shaped by appropriate choices of resistor and capacitor values. A schematic of the circuit design is shown in Fig. 6. The filter response for this application was designed to be a low-pass filter with a slight notch near 3 kHz.<sup>21</sup> The predicted and measured controller responses are shown in Fig. 7. The slight discrepancies between the two curves are due to the tolerances associated with the resistor and capacitor components used in the actual circuit.

The two control circuits were implemented on an electrical breadboard. National Semiconductor LM837N quad operational amplifier chips were used; three out of the four op-amps on the chip were needed for each control circuit. The output of each accelerometer was fed to the input of a control circuit while the output of each control circuit was passed through one channel of a two-channel variable-gain Crown DC300A power amplifier. The amplifier was used to

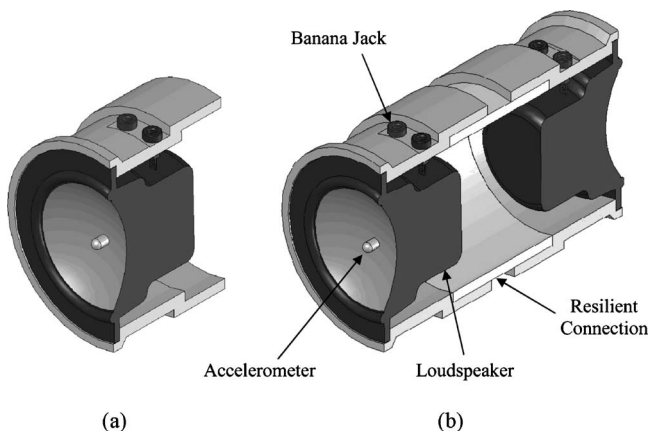


FIG. 4. Cutaway diagram of the ASP module for (a) an active single-panel partition and (b) an active double-panel partition (right).

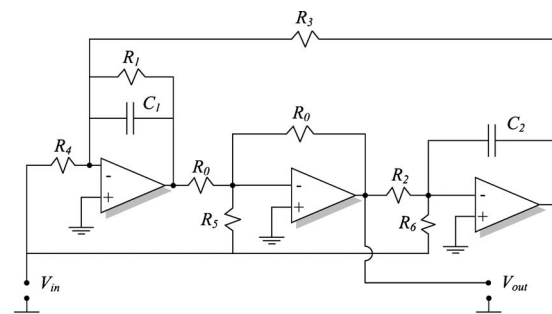


FIG. 6. Electrical schematic for a second-order Fleischer-Tow biquad circuit.

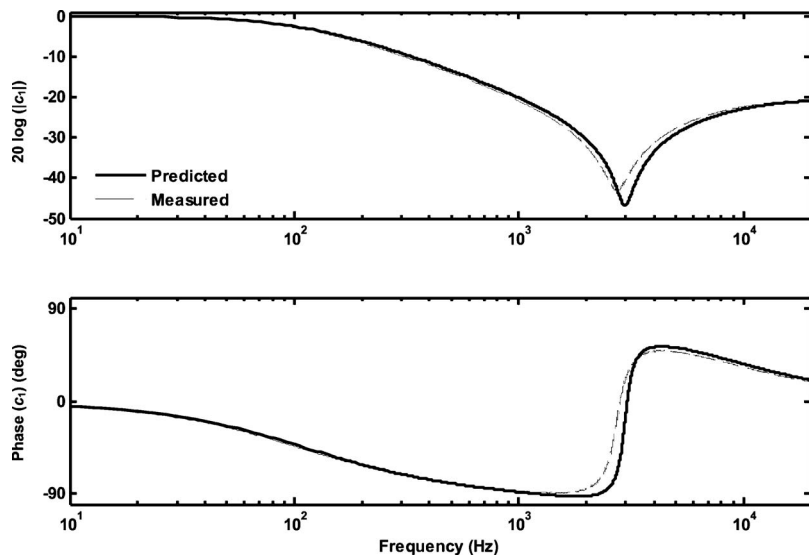


FIG. 7. Predicted and measured controller FRFs for a Fleischer-Tow biquad controller.

adjust the gain of each controller. Finally, the respective output of the amplifier was fed to a loudspeaker in the active partition module.

### III. RESULTS

#### A. Plant accelerance FRFs

The accelerance FRF (the acceleration output divided by the voltage input) of the plant was predicted using the enhanced double-panel TL model described in Ref. 21 and the values given in Table I. The predicted and measured plant responses are shown in Fig. 8. The former was based on the assumption of anechoic plane-wave loading on both sides of the module and has been normalized. The latter was measured in free air (without tube loading), although the difference with tube loading was insignificant. The model matches the measured data very well up to 2 kHz. However the assumptions of lumped-parameter behavior break down above 2 kHz, when the cone (with the mounted accelerometer) begins to exhibit strong modal resonance. As suggested by the figure, the model prediction is useful for making design decisions affecting the low-frequency response and stability,

but the *measured* frequency response function is needed to account for the unpredicted high-frequency dynamics of the plant. One of the advantages to the controller chosen for the research was its incorporation of a notch filter strategically centered at 3 kHz to mitigate the unpredicted resonant response from the closed-loop system. It did so by significantly reducing the excitation voltage feeding the loudspeaker near this frequency.

#### B. Acoustic coupling FRFs

The acoustic coupling FRF of the plant was also predicted using the enhanced double-panel TL model in Ref. 21. The predicted and free-air-measured FRFs are shown in the normalized plots of Fig. 9. Again, the model provides very good predictions of the strength of the acoustic coupling path at low frequencies. As is expected in a double-panel partition, the strength of the acoustic coupling is greatest at the mass-air-mass resonance frequency, which is 155 Hz for this module. The strength of the acoustic coupling rises at 12 dB

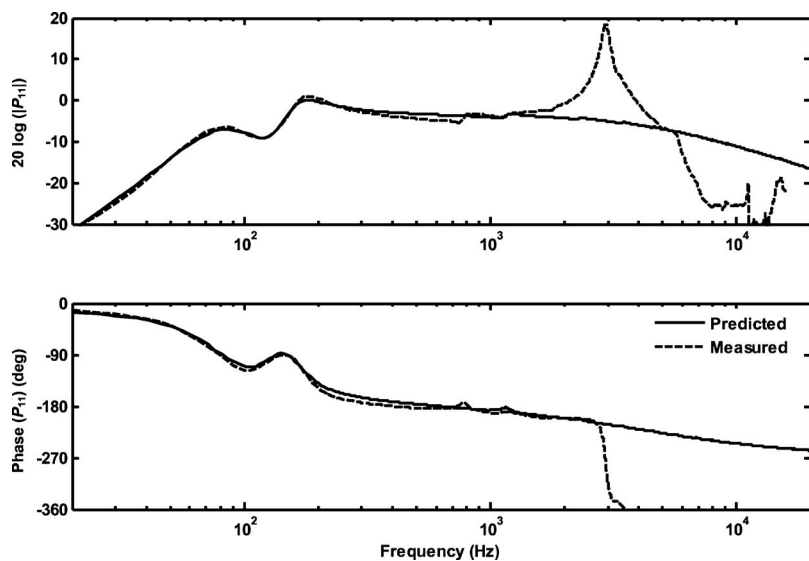


FIG. 8. Predicted and measured plant accelerance FRFs.

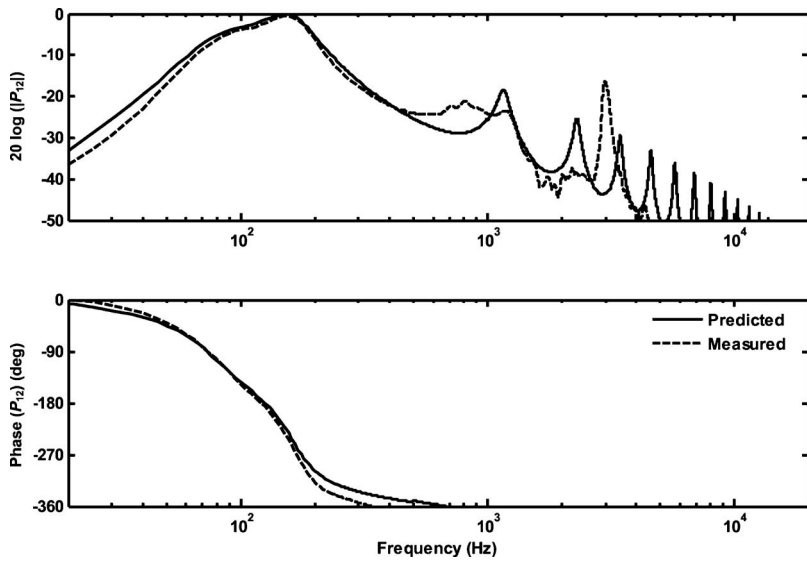


FIG. 9. Predicted and measured cross-coupling acceleration FRFs.

per octave well below the mass-air-mass resonance frequency, 6 dB per octave in the immediate vicinity, and falls at 18 dB per octave immediately above it.

The acoustic coupling works in favor of the control scheme used in the module. Suppose a disturbance wave is incident upon the first panel of the partition. If the panel is set into vibratory motion, the acoustic coupling will cause the second panel to vibrate. The amplitude at which the second panel vibrates depends on the magnitude of the acoustic coupling. Consequently, if the first panel is actively controlled so that it cannot vibrate, the acoustic coupling will force the second panel to follow suit. Likewise, active control of the second panel will encourage the first panel to follow suit. The panels tend to act more independently at frequencies where the acoustic coupling is not so strong.

### C. Transmission loss

The TL was predicted and measured for several different module configurations and excitation schemes. The first involved a single-driver module (i.e., as a single-panel partition) with an excitation source on its source (upstream) side.

The second involved a two-driver module (i.e., as a double-panel partition) with the same excitation. The last again involved the two-driver module, but with excitation sources on both the source and receiving sides. The downstream source included a driver and enclosure similar to that of the upstream source, but it was side mounted to the tube before the anechoic termination using a T-section. The TL results for each scheme are presented in the following sections and compared to the model predictions developed in Ref. 21.

#### 1. Single-panel partition results

The single-panel partition was produced by removing the second driver from the module as shown in Fig. 4(a). It was oriented so the cone of the loudspeaker was facing the excitation source. The TL was measured for both passive and active states. The predicted and measured TL curves are plotted in Fig. 10. The measurement bandwidth is restricted to 2 kHz because the measurement was made in the plane-wave tube apparatus.

The measured TLs agree reasonably well with the predicted TLs up to frequencies approaching 1 kHz. The mea-

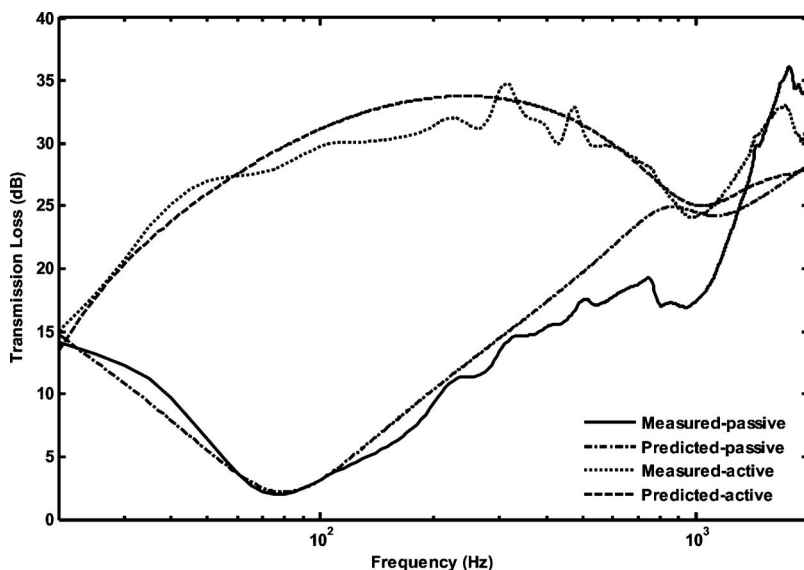
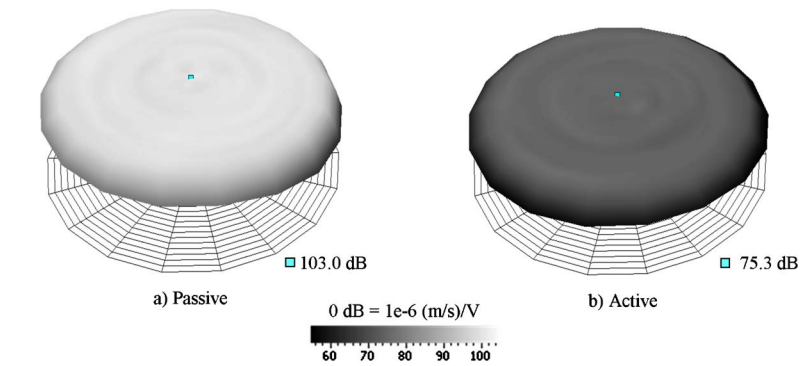


FIG. 10. Predicted and measured TL of a single-panel partition in passive and active states.

RMS surface velocity at 100 Hz



RMS surface velocity at 1000 Hz

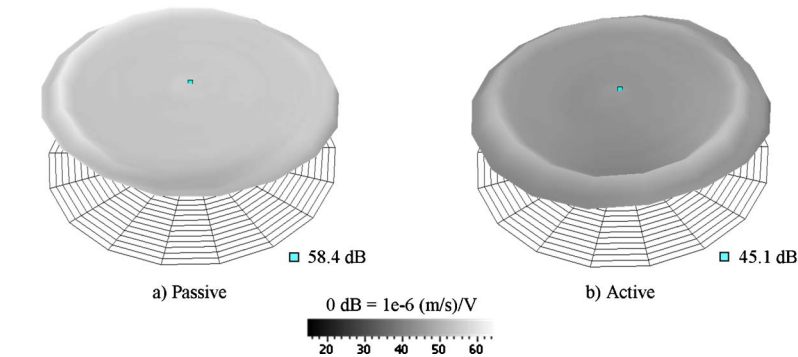


FIG. 11. (Color online) Scanning laser Doppler vibrometer measurements of the RMS surface velocities for driver cone of a single-panel partition at 100 Hz and 1 kHz in passive and active control states. The decibel values provided for each case are the measured values near the center of the cone. They provide an indication of the vibration levels with and without active control.

sured passive TL does not perform as well as anticipated in the region right around 1 kHz, but it performs better than expected at higher frequencies. These discrepancies occur in the region where the surround moves out of phase with the cone through a higher-order resonance (i.e., the second resonance of the two-degree-of-freedom cone/surround system within the module configuration). Although the model does represent the separate surround motion and its mechanical coupling to the cone, it does not fully account for the self and mutual radiation impedances between the two surfaces. Nor does it account for the various constricted paths through and around the driver assembly. These deficiencies may partly explain the discrepancies, but further investigation is required.

The expected degradation in the active TL near 1 kHz is caused by two separate phenomena. The first is due to slight control instability in the region. The phase of the closed-loop system crosses the  $-360^\circ$  point at 1 kHz causing a small amplification of the disturbance signal to occur at this frequency. The second is again due to the surround moving independently with a resonance near 1 kHz. The effect cannot be actively controlled because there is no way to simultaneously actuate the surround area. This was verified by scanning the face of the panel with a scanning laser Doppler vibrometer in both the passive and active states. The scan results are shown at 100 Hz and 1 kHz in Fig. 11. The surround resonance effect is clearly seen under active control at 1 kHz but not at 100 Hz.

## 2. Double-panel partition results

The double-panel partition was configured as shown in Fig. 4(b). The TL was measured for both passive and active

module states. Three different active control states were possible: active control of panel 1 only, active control of panel 2 only, and active control of both panels simultaneously. The predicted and measured TL curves are plotted in Fig. 12.

The experimental results agree reasonably well with the model predictions over a broad frequency range. However, one obvious discrepancy involves the strength of the dominant cavity resonance near 1.15 kHz. The corresponding TL dip does appear in the measured data, but it is less severe than anticipated because the model fails to account for all module damping. The interconnected acoustic elements behind the loudspeaker cone are much more complicated than the simple model suggests. Circuitous paths through and around the driver assembly and within the module housing are not well represented. The driver incorporates several orifices in the basket and coil former. Its mounting in the module housing also introduces several constricted transmission paths. Both the orifices and constrictions would add acoustic mass and resistance to the model.<sup>26</sup> The spider likewise adds acoustic resistance. As has been shown recently for the same driver and a similar mounting,<sup>27</sup> measurements of the acoustic loading beyond the cone tend to show greater losses than anticipated with a simple driver and cavity model. Elaboration of the model is beyond the scope of this paper.

It was interesting to observe that the module TL performance was essentially identical when only panel 1 or panel 2 was actively controlled. This indicates that it does not matter whether the disturbing sound wave first interacts with a passive panel or an active panel, as long as one of the two panels is actively controlled. However, the mass-air-mass resonance dip near 150 Hz remains in either case. It is completely eliminated when both panels are controlled simultaneously.

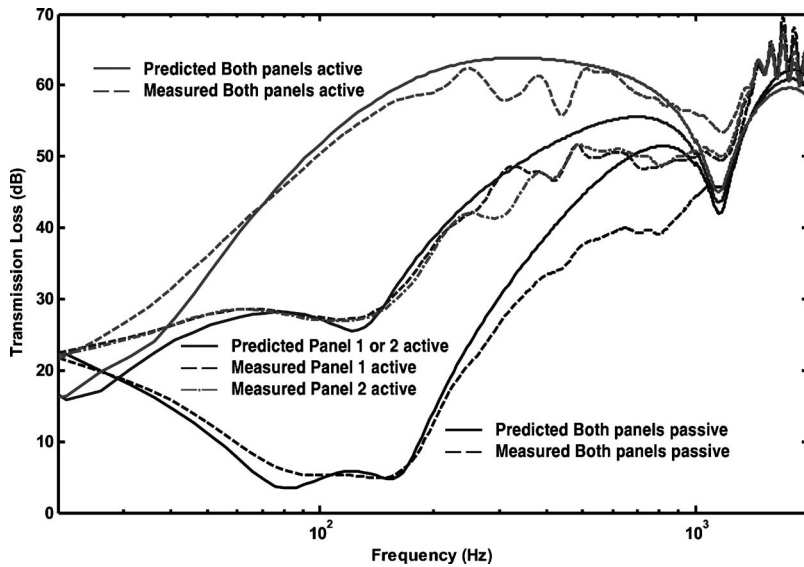


FIG. 12. Predicted and measured TL of a double-panel partition in passive and active states.

The arithmetic average TL (both measured and predicted) between 20 Hz and 1 kHz was computed for the single- and double-panel partitions in all of their control states. The results are shown in Table II. They reveal that the active panel control can provide effective broadband TL, even in the single-panel case. However, the double-panel module with active control on both panels provides the most substantial increase in the broad, low-frequency TL performance.

The maximum increase in TL from the passive state to the active state of each module was also computed from both the measured and predicted data. The results are shown in Table III. The increase is substantial for both the single-panel and double-panel partitions. Actively controlling both panels of the double-panel partition effectively doubles the maximum TL increase (in dB) of the module over actively controlling only a single panel of the double-panel partition.

### 3. Bidirectional results

Broadband bidirectional TL is not possible to measure using conventional testing techniques. The presence of a second excitation source on the receiving side of the measurement apparatus simply acts to degrade the measured TL through the module. However, a simple test provides some insight into the bidirectional capabilities of the module. Two

distinct tones were used to ensure the module could attenuate in either direction as the sounds passed through it—even if the tones were present at the same time.

In order to carry out this experiment, a side-branch T-section was added to the receiving-side tube of the measurement apparatus in Fig. 1 to enable the use of a downstream excitation source. The upstream source radiated a 75 Hz tone and the downstream source radiated a 150 Hz tone. The sound pressure level (SPL) was measured with two microphones, one located in the central region of the source-side tube, and one located in the central region between the module and the downstream source. The difference in SPL ( $\Delta$ SPL) between the two microphones in the direction of sound propagation for the tone was used as a rough qualitative means of evaluating the module sound isolation for these long-wavelength cases. The results for the double-panel partition are shown in Table IV. The values for the expected TL came from Fig. 12 at 75 and 150 Hz.

The first observation from the table is the already suggested fact that the  $\Delta$ SPL is not as good a quantitative metric as the TL. One reason for this is that the SPL in the upstream tube is a strong function of position and frequency due to its axial modes and resonances. However, the measured attenuation in SPL was still comparable to the predicted TL. The

TABLE II. Arithmetic average TL between 20 and 1000 Hz for the single- and double-panel partitions in each control state.

	Measured average TL (20–1000 Hz) (dB)	Predicted average TL (20–1000 Hz) (dB)
Single-panel, passive	14	11
Single-panel, active	29	31
Double-panel, passive	31	37
Double-panel, panel 1 active	45	48
Double-panel, panel 2 active	45	48
Double-panel, both panels active	57	58

TABLE III. Maximum increase in TL from passive to active states for the single- and double-panel partitions in each control state.

	Maximum measured increase in TL from passive to active state (dB @ Hz)	Maximum predicted increase in TL from passive to active state (dB @ Hz)
Single-panel, passive	N/A	N/A
Single-panel, active	27 @ 95	28 @ 95
Double-panel, passive	N/A	N/A
Double-panel, panel 1 active	26 @ 175	27 @ 165
Double-panel, panel 2 active	25 @ 155	27 @ 165
Double-panel, both panels active	52 @ 160	55 @ 160

TABLE IV. Bidirectional sound isolation results for two tones passing through the module in different directions.

	$\Delta$ SPL (dB)	Expected TL (dB)
	Passive	
75 Hz	13	7
150 Hz	12	5
	Panel 1 active	
75 Hz	33	28
150 Hz	31	29
	Panel 2 active	
75 Hz	33	28
150 Hz	31	29
	Both panels active	
75 Hz	48	45
150 Hz	50	57

second and more important observation is that the module can provide the same attenuation when sound is propagating in both directions through the module as it can when sound is only propagating in one direction through the module.

### D. Electrical power consumption

The increase in the TL from passive to active states comes at the expense of electrical power consumption. A natural question to ask is how much power the active module requires relative to the sound power that is incident upon it. The total electrical power was predicted from the steady-state voltage and current supplied to the double-panel module for each control case. The total incident sound power was also measured for each case using the two-microphone transfer-function technique. The electrical power was then divided by the incident sound power to form a power ratio.

When only a single panel was actuated at a time, panel 1 used almost twice the power as panel 2. However, the same TL is achieved by controlling either panel 1 or panel 2 alone. This indicates that the passive TL characteristics within the module are not fully leveraged if the first panel of a unidirectional transmission path is actuated. Consequently, if foreknowledge about the direction of sound transmission through the device is available, it would be more efficient to actuate the second panel in the transmission path.

The best TL performance was achieved when both panels were actively controlled. This scheme consumed only slightly more power than controlling panel 1 alone, while it nearly doubled the TL performance of the module in decibels. An electrical to acoustic power ratio of 3 was calculated for this case.

### IV. CONCLUSIONS

This work has validated the modeling of a proposed double-panel module for use in active segmented partitions (ASPs). It has shown experimentally that direct-panel vibration control of the module using analog feedback controllers provides an effective way to produce high transmission loss

(TL) of random disturbances over a broad frequency band. The TL performance was substantially increased by actuating both panels instead of one, while requiring only slightly more electrical power than when actively controlling the first panel alone. For the fully active case, the average TL from 20 Hz to 1 kHz was 57 dB, whereas the average passive TL for the same device was only 31 dB over the same bandwidth. The work also demonstrated that the module provides bidirectional TL control. Electrical power consumption of the fully active device was estimated under certain measurement conditions and found to produce a ratio of electrical power to incident sound power of approximately 3:1.

### ACKNOWLEDGMENTS

The authors gratefully acknowledge financial support from the Department of Mechanical Engineering at Brigham Young University as well as the NASA Rocky Mountain Space Grant Consortium.

- <sup>1</sup>F. Fahy, *Sound and Structural Vibration: Radiation, Transmission, and Response* (Academic, London, 1985).
- <sup>2</sup>D. A. Bies and C. H. Hansen, *Engineering Noise Control: Theory and Practice* (Unwin Hyman, London, 1988).
- <sup>3</sup>C. R. Fuller and R. J. Silcox, "Acoustics 1991: Active structural acoustic control," *J. Acoust. Soc. Am.* **91**, 519 (1992).
- <sup>4</sup>C. R. Fuller, C. H. Hansen, and S. D. Snyder, "Active control of sound radiation from a vibrating rectangular panel by sound sources and vibration inputs: An experimental comparison," *J. Sound Vib.* **145**, 195–215 (1991).
- <sup>5</sup>D. R. Thomas, P. A. Nelson, S. J. Elliott, and R. J. Pinnington, "Experimental investigation into the active control of sound transmission through stiff light composite panels," *Noise Control Eng. J.* **41**, 273–279 (1993).
- <sup>6</sup>B. Bingham, M. J. Atalla, and N. W. Hagood, "Comparison of structural-acoustic control designs on an active composite panel," *J. Sound Vib.* **244**, 761–778 (2001).
- <sup>7</sup>S. M. Hirsch, N. E. Meyer, M. A. Westervelt, P. King, F. J. Li, M. V. Petrova, and J. Q. Sun, "Experimental study of smart segmented trim panels for aircraft interior noise control," *J. Sound Vib.* **231**, 1023–1037 (2000).
- <sup>8</sup>S. M. Hirsch, J. Q. Sun, and M. R. Jolly, "Analytical study of interior noise control using segmented panels," *J. Sound Vib.* **231**, 1007–1021 (2000).
- <sup>9</sup>M. E. Johnson and S. J. Elliott, "Active control of sound radiation using volume velocity cancellation," *J. Acoust. Soc. Am.* **98**, 2174–2186 (1995).
- <sup>10</sup>B. Petitjean, I. Legrain, F. Simon, and S. Pausin, "Active control experiments for acoustic radiation reduction of a sandwich panel: Feedback and feedforward investigations," *J. Sound Vib.* **252**, 19–36 (2002).
- <sup>11</sup>R. L. St. Pierre, Jr., G. H. Koopman, and W. Chen, "Volume velocity control of sound transmission through composite panels," *J. Sound Vib.* **210**, 441–460 (1998).
- <sup>12</sup>E. Bianchi, P. Gardonio, and S. J. Elliott, "Smart panel with multiple decentralized units for the control of sound transmission. Part III: Control system implementation," *J. Sound Vib.* **274**, 215–232 (2004).
- <sup>13</sup>P. Gardonio, E. Bianchi, and S. J. Elliott, "Smart panel with multiple decentralized units for the control of sound transmission. Part I: Theoretical predictions," *J. Sound Vib.* **274**, 163–192 (2004).
- <sup>14</sup>P. Gardonio, E. Bianchi, and S. J. Elliott, "Smart panel with multiple decentralized units for the control of sound transmission. Part II: Design of the decentralized control units," *J. Sound Vib.* **274**, 193–213 (2004).
- <sup>15</sup>T. W. Leishman, "Active control of sound transmission through partitions composed of discretely controlled modules," Ph.D. thesis, The Pennsylvania State University, University Park, PA (2000).
- <sup>16</sup>T. W. Leishman and J. Tichy, "A fundamental investigation of the active control of sound transmission through segmented partition elements," in *Proceedings of the INCE Conference (1997)*, Vol. **103**, pp. 137–148.
- <sup>17</sup>T. W. Leishman and J. Tichy, "A theoretical and numerical analysis of vibration-controlled modules for use in active segmented partitions," *J. Acoust. Soc. Am.* **118**, 1424–1438 (2005).
- <sup>18</sup>T. W. Leishman and J. Tichy, "An experimental investigation of two mod-

- ule configurations for use in active segmented partitions,” *J. Acoust. Soc. Am.* **118**, 1439–1451 (2005).
- <sup>19</sup>T. W. Leishman and J. Tichy, “An experimental investigation of two active segmented partition arrays,” *J. Acoust. Soc. Am.* **118**, 3050–3063 (2005).
- <sup>20</sup>J. D. Sagers, “Analog feedback control of an active sound transmission control module,” MS thesis, Brigham Young University, Provo, UT (2007).
- <sup>21</sup>J. D. Sagers, T. W. Leishman, and J. D. Blotter, “A double-panel active segmented partition using decoupled analog feedback controllers: Numerical model,” *J. Acoust. Soc. Am.* **125**, 3806–3818 (2009).
- <sup>22</sup>J. Y. Chung and D. A. Blaser, “Transfer function method of measuring in-duct acoustic properties, Part I: Theory,” *J. Acoust. Soc. Am.* **68**, 907–913 (1980).
- <sup>23</sup>J. Y. Chung and D. A. Blaser, “Transfer function method of measuring in-duct acoustic properties, Part II: Experiment,” *J. Acoust. Soc. Am.* **68**, 914–921 (1980).
- <sup>24</sup>H. Bodén and M. Åbom, “Influence of errors on the two-microphone method for measuring acoustic properties in ducts,” *J. Acoust. Soc. Am.* **79**, 541–549 (1986).
- <sup>25</sup>P. E. Fleischer and J. Tow, “Design formulas for biquad active filters using three operational amplifiers,” *Proc. IEEE* **61**, 662–663 (1973).
- <sup>26</sup>P. M. Morse and K. U. Ingard, *Theoretical Acoustics* (Princeton University Press, Princeton, NJ, 1987).
- <sup>27</sup>X. Chen, “Equalization of loudspeakers and enclosed sound fields,” Ph.D. thesis, Brigham Young University, Provo, UT (2009).